ELSEVIER

Computer Aided Geometric Design 19 (2002) 257–273

COMPUTER AIDED GEOMETRIC DESIGN

www.elsevier.com/locate/comaid

Shape-preserving, multiscale interpolation by univariate curvature-based cubic L_1 splines in Cartesian and polar coordinates

John E. Lavery

Mathematics Division, Army Research Office, Army Research Laboratory , P.O. Box 12211, Research Triangle Park, NC 27709-2211, USA

Received 1 March 2001; received in revised form 1 November 2001

Abstract

We investigate C^1-smooth univariate curvature-based cubic L_1 interpolating splines in Cartesian and polar coordinates. The coefficients of these splines are calculated by minimizing the L_1 norm of curvature. We compare these curvature-based cubic L_1 splines with second-derivative-based cubic L_1 splines and with cubic L_2 splines based on the L_2 norm of curvature and of the second derivative. In computational experiments in Cartesian coordinates, cubic L_1 splines based on curvature preserve the shape of multiscale data well, as do cubic L_1 splines based on the second derivative. Cartesian-coordinate cubic L_1 splines preserve shape much better than analogous Cartesian-coordinate cubic L_2 splines. In computational experiments in polar coordinates, cubic L_1 splines based on curvature preserve the shape of multiscale data better than cubic L_1 splines based on the second derivative and much better than analogous cubic L_2 splines. Extensions to splines in general curvilinear coordinate systems, to bivariate splines in spherical coordinate systems and to nonpolynomial splines are outlined. Published by Elsevier Science B.V.

Keywords: Cartesian coordinates; Cubic spline; Curvature; Interpolation; L_1 spline; L_2 spline; Multiscale; Polar coordinates; Shape preservation; Univariate

1. Introduction

In a classical framework, a univariate cubic spline $z(x)$ in Cartesian coordinates is calculated by minimizing the integral of the square of the second derivative z'' of the spline. The rationale for using z''

E-mail address: lavery@aro.arl.army.mil (J.E. Lavery).

0167-8396/02/$ – see front matter Published by Elsevier Science B.V.
PII: S0167-8396(02)00087-0

in the minimization principle is that it results in a linear problem and, for first derivatives z' of small absolute value, the second derivative z'' is a good approximation of the curvature

$$\kappa = \frac{z''}{[1 + (z')^2]^{3/2}}. \tag{1}$$

However, when multiscale data, that is, data with abrupt changes in magnitude and spacing, for which $|z'|$ can be arbitrarily large, is under consideration, ignoring the denominator in the expression for curvature biases the problem. In regions where $|z'|$ is large, the "linearized curvature" z'' is much larger in absolute value than the true curvature (1). As a result, a classical spline is constructed using inordinately large weight on the steep portions of the spline and relatively less weight on the flat portions. In part because of this, a classical spline inevitably has Gibbs phenomena (extraneous over/undershoot) near multiscale phenomena and does not preserve the shape of the data.

Many methods, including adjusting the positions of nodes, introducing additional nodes, adding constraints and/or penalties such as curvature weighting/control, a posteriori filtering and fairing, have been used with considerable success to increase the shape-preserving properties of classical splines. However, none of these methods preserves shape for multiscale data without human interaction. Recently, univariate and bivariate L_1 splines, that is, splines constructed by minimizing the L_1 norm of the second derivatives, have been shown to be effective at preserving the shape of multiscale data in Cartesian coordinate systems without requiring adjustment of nodes, constraints, penalties, filtering, fairing or human interaction (Lavery, 2000, 2001).

Interpolation in curvilinear coordinate systems is a topic of active research, one in which the goal of achieving shape-preserving representation of data by computationally simple smooth curves and surfaces is more challenging than it is in Cartesian coordinate systems. A fundamental issue in all curvilinear coordinate systems is "curvilinear warping", that is, the inherent nonzero curvature of the space. Many types of splines for polar coordinate systems have been investigated, including polynomial splines (Golomb, 1968; Schumaker, 1981; Goodman and Lee, 1984; Alfeld et al., 1995), trigonometric splines (Lyche and Winther, 1979; Schumaker, 1981; Goodman and Lee, 1984; Lyche, 1999) and splines based on reciprocals of trigonometric functions (Sanchez-Reyes, 1992; de Casteljau, 1994; Casciola and Morigi, 1997). However, shape preservation by splines in polar and, more generally, in curvilinear coordinate systems can typically be achieved only with considerable human interaction.

Work on splines in curvilinear coordinate systems has been carried out by one community of committed researchers. Curvature-based splines have been a topic of interest to another, smaller community of equally committed researchers. "Minimum-curvature" splines, which are based on minimizing the square of curvature, have been investigated in (Jerome, 1973a, 1973b, 1975; Fisher and Jerome, 1976; Golomb and Jerome, 1982; Burmeister et al., 1985; Linner, 1996). These splines have been of considerable interest in locating closed geodesics, curve straightening and modeling thin elastic rods. Use of curvature-based splines for shape-preserving modeling of multiscale data in Cartesian or curvilinear coordinate systems has, however, not been a major objective of past research.

We foresee advantages in linking curvature-based splines with modeling of multiscale data, especially in curvilinear coordinate systems. The hypothesis underlying this paper is that cubic L_1 splines constructed by minimizing the L_1 norm of the curvature are computationally feasible and preserve shape well in both Cartesian and polar coordinate systems. Our focus here will be on univariate cubic L_1 splines. We will compare these curvature-based cubic L_1 splines with second-derivative-based cubic L_1 splines and with cubic splines based on the L_2 norm of curvature and of the second derivative.

There is a widespread perception that univariate interpolation is a well understood and practically closed subject, perhaps in part because of the pressing need for bi- and multivariate geometric representation. We feel that there is value in returning to research on univariate interpolation to achieve fundamentally new understanding. We carry out our univariate investigation in a framework that leads directly to bi- and multivariate extensions, which we outline in Section 7.

Throughout this paper, ε denotes a small positive number.

2. Cubic L_1 and L_2 splines in Cartesian coordinates

Cartesian-coordinate cubic L_1 and L_2 splines based on the second derivative were defined and investigated in (Lavery, 2000). In this section, we first discuss those splines, which we designate "Cartesian second derivative cubic splines". We then introduce cubic L_1 and L_2 splines based on curvature, which we designate "Cartesian curvature cubic splines". The Cartesian-coordinate splines considered in this paper have no boundary conditions. Periodic, fixed-derivative or other boundary conditions could be imposed on these splines with no significant change in the theory or computational methods.

All of the Cartesian-coordinate splines in this paper will be on a grid consisting of a strictly monotonic but otherwise arbitrary partition of the finite real interval $[x_0, x_I]$:

$$-\infty < x_0 < x_1 < x_2 < \cdots < x_{I-1} < x_I < \infty. \tag{2}$$

The task is to interpolate the data $\{(x_i, z_i)\}_{i=0}^{I}$. In each interval (x_i, x_{i+1}), $i = 0, 1, \ldots, I-1$, a piecewise cubic interpolant z can be expressed as a Hermite-type function using the data z_i, z_{i+1} and the first derivatives $b_i = \mathrm{d}z(x_i)/\mathrm{d}x$, $b_{i+1} = \mathrm{d}z(x_{i+1})/\mathrm{d}x$ at the endpoints of the interval:

$$\begin{aligned} z(x) \;=\; & z_i + b_i(x - x_i) + \frac{1}{h_i}\big[-(2b_i + b_{i+1}) + 3\Delta z_i\big](x - x_i)^2 \\ & + \frac{1}{h_i^2}[b_i + b_{i+1} - 2\Delta z_i](x - x_i)^3 \end{aligned} \tag{3}$$

where

$$h_i := x_{i+1} - x_i \tag{4}$$

and

$$\Delta z_i := \frac{z_{i+1} - z_i}{h_i}. \tag{5}$$

Calculating a Cartesian-coordinate cubic spline consists of calculating the first derivatives b_i of the spline at the nodes by minimizing one of the functionals described in the remainder of this section.

2.1. Cartesian second derivative splines

We define a "Cartesian second derivative L_p spline", that is, a Cartesian-coordinate cubic L_p spline, $1 \leqslant p < \infty$, based on the second derivative, to be a piecewise cubic polynomial that minimizes

$$\int_{x_0}^{x_I} \left| \frac{\mathrm{d}^2 z}{\mathrm{d}x^2} \right|^p \mathrm{d}x \tag{6}$$

over all piecewise cubic polynomials z that interpolate the data and have continuous derivatives at the nodes x_i. When $p = 1$, regularization terms are added—see below. This definition coincides with the definition of L_p splines in (Lavery, 2000).

The p of interest here are $p = 1$ and $p = 2$. L_2 splines defined by minimization of (6) exist, are unique and coincide with conventional cubic splines. L_1 splines defined by minimization of (6) exist are not necessarily unique. To alleviate this problem, one can add "regularization" terms to the minimization principle to make it

$$\int_{x_0}^{x_I} \left| \frac{\mathrm{d}^2 z}{\mathrm{d}x^2} \right| \mathrm{d}x + \varepsilon \sum_{i=0}^{I} \left| \frac{\mathrm{d}z}{\mathrm{d}x}(x_i) \right|. \tag{7}$$

(As mentioned at the end of the Introduction, ε is a small positive number.) Functional (7) is still not strictly convex and can therefore achieve its minimum for more than one set of spline coefficients. However, standard interior-point algorithms, including the primal affine method used to generate computational results in the present paper and in (Lavery, 2000), do yield a unique set of spline coefficients that minimize (a discretization of) functional (7).

2.2. Cartesian curvature splines

In the research literature and in operational codes, cubic splines based on curvature previously have been defined using the arclength integral of the square of curvature. Adopting this tradition, we define a "Cartesian curvature L_2 spline of type 1" to be a piecewise cubic polynomial that minimizes

$$\int_{x=x_0}^{x=x_I} (\kappa)^2 \,\mathrm{d}s \tag{8}$$

over all piecewise cubic polynomials z that interpolate the data and have continuous derivatives at the nodes x_i. Here and throughout this paper, $\mathrm{d}s$ is the arclength differential

$$\mathrm{d}s = \left[1 + (z')^2\right]^{1/2} \mathrm{d}x. \tag{9}$$

Functional (8) can be rewritten using (1) and (9) as

$$\int_{x_0}^{x_I} \frac{(z'')^2}{[1 + (z')^2]^{5/2}} \,\mathrm{d}x. \tag{10}$$

Golomb and Jerome (1982) have carried out a global and local analysis of minimization of functional (10) or, equivalently, (8) over an infinite-dimensional space of smooth functions. They give theorems on well-posedness and uniqueness and derive sharp characterizations for the resulting splines. Analysis of minimization of (8) over the finite-dimensional space of C^1-smooth cubic functions of interest in this paper has not yet been carried out. Such an analysis is beyond the scope of the present paper, which is oriented toward providing the evidence that carrying out that analysis is likely to have high value. The analysis of minimization of (8) over the finite-dimensional space of C^1-smooth cubic interpolating functions should be carried out in the context of analysis of all of the L_2 and L_1 curvature-based functionals mentioned below in this subsection and in Subsection 3.2.

While precise conditions for local or global existence and uniqueness of the minimum of (8) are not known, it is known that adding a strictly convex expression to this or any functional enhances existence, uniqueness and computational stability. For this reason, we choose to add to functional (8) strictly convex regularization terms that are squared analogues of the regularization terms that were added above in functional (7) to obtain

$$\int_{x=x_0}^{x=x_I} (\kappa)^2 \,\mathrm{d}s + \varepsilon^2 \sum_{i=0}^{I} \left(\frac{\mathrm{d}z}{\mathrm{d}x}(x_i) \right)^2 \tag{11}$$

or, equivalently,

$$\int_{x_0}^{x_I} \frac{(z'')^2}{[1+(z')^2]^{5/2}} \,\mathrm{d}x + \varepsilon^2 \sum_{i=0}^{I} \left(\frac{\mathrm{d}z}{\mathrm{d}x}(x_i) \right)^2. \tag{12}$$

Functional (11) or (12) may, of course, still have more than one local minimum and therefore result in more than one set of spline coefficients. However, in all of the computational experiments carried out by the author, the variant of the Levenberg–Marquardt method (Dennis and Schnabel, 1983; Press et al., 1988) used to generate the Cartesian curvature-based L_2 spline computational results in this paper yielded a unique set of spline coefficients that minimize (a discretization of) functional (12).

For a reason explained in the note at the end of this section, we define a "Cartesian curvature L_2 spline of type 2" to be a C^1-smooth piecewise cubic interpolant that minimizes

$$\int_{x_0}^{x_I} \frac{(z'')^2}{[1+(z')^2]^2} \,\mathrm{d}x + \varepsilon^2 \sum_{i=0}^{I} \left(\frac{\mathrm{d}z}{\mathrm{d}x}(x_i) \right)^2. \tag{13}$$

Let us now define L_1 analogues of the Cartesian curvature L_2 splines introduced above. Taking the square roots of the integrand, ε^2 and the summand in functional (12), we define a "Cartesian curvature L_1 spline of type 1" to be a C^1-smooth piecewise cubic interpolant that minimizes

$$\int_{x_0}^{x_I} \frac{|z''|}{[1+(z')^2]^{5/4}} \,\mathrm{d}x + \varepsilon \sum_{i=0}^{I} \left| \frac{\mathrm{d}z}{\mathrm{d}x}(x_i) \right|. \tag{14}$$

(One could create a different analogue of Cartesian curvature L_2 splines by taking the square roots of the integrand, ε^2 and the summand in functional (11).) We define a "Cartesian curvature L_1 spline of type 2" to be a C^1-smooth piecewise cubic interpolant that minimizes

$$\int_{x=x_0}^{x=x_I} |\kappa| \,\mathrm{d}s + \varepsilon \sum_{i=0}^{I} \left| \frac{\mathrm{d}z}{\mathrm{d}x}(x_i) \right| \tag{15}$$

or, equivalently,

$$\int_{x_0}^{x_I} \frac{|z''|}{1+(z')^2} \,\mathrm{d}x + \varepsilon \sum_{i=0}^{I} \left| \frac{\mathrm{d}z}{\mathrm{d}x}(x_i) \right|. \tag{16}$$

Local and global existence and uniqueness properties of Cartesian curvature L_1 splines are not yet known. Functionals (14) and (16) may each have more than one local minimum. However, in all of the computational experiments carried out by the author, the primal-affine-type method used to generate the Cartesian curvature L_1 spline computational results in this paper yielded unique sets of spline coefficients that minimize (discretizations of) functionals (14) and (16).

Note. Cartesian curvature L_2 splines of type 2 were introduced above because they are L_2 analogues of Cartesian curvature L_1 splines of type 2.

3. Cubic L_1 and L_2 splines in polar coordinates

Polar-coordinate cubic splines based on the second derivative have been common in the literature. In this section, we first discuss the conventional variety of these splines, which we designate "polar second derivative L_2 splines". We then introduce "polar second derivative L_1 splines". Finally, we define four types of "polar curvature L_1 and L_2 splines". The polar-coordinate splines considered in this paper have periodic boundary conditions. Fixed-derivative or other boundary conditions or no boundary conditions at all could be imposed on these splines with no significant change in the theory or computational methods.

All of the polar-coordinate splines in this paper will be on a periodic spline grid consisting of a strictly monotonic but otherwise arbitrary partition of the periodic real interval $[\theta_0, \theta_0 + 2\pi]$:

$$\theta_0 < \theta_1 < \theta_2 < \cdots < \theta_{I-1} < \theta_I = \theta_0 + 2\pi. \tag{17}$$

The task is to interpolate the periodic data $\{(\theta_i, r_i)\}_{i=0}^{I}$, where $r_i > 0\ \forall i$ and $r_I = r_0$. In each interval (θ_i, θ_{i+1}), $i = 0, 1, \ldots, I-1$, a piecewise cubic interpolant can be expressed as a Hermite-type function using the data r_i, r_{i+1} and the first derivatives $b_i = \mathrm{d}r(\theta_i)/\mathrm{d}\theta$, $b_{i+1} = \mathrm{d}r(\theta_{i+1})/\mathrm{d}\theta$ at the endpoints of the interval:

$$\begin{aligned} r(x) \;&=\; r_i + b_i(\theta - \theta_i) + \frac{1}{h_i}\big[-(2b_i + b_{i+1}) + 3\Delta r_i\big](\theta - \theta_i)^2 \\ &\quad + \frac{1}{h_i^2}[b_i + b_{i+1} - 2\Delta r_i](\theta - \theta_i)^3 \end{aligned} \tag{18}$$

where

$$h_i := \theta_{i+1} - \theta_i \tag{19}$$

and

$$\Delta r_i := \frac{r_{i+1} - r_i}{h_i}. \tag{20}$$

Calculating a polar-coordinate cubic spline consists of calculating the first derivatives b_i of the spline at the nodes by minimizing one of the functionals described in the remainder of this section.

3.1. Polar second derivative splines

In the prior literature and in practical implementations, it has been most common to define a polar-coordinate spline to be a function that minimizes

$$\int_{\theta_0}^{\theta_I} \left(\frac{\mathrm{d}^2 r}{\mathrm{d}\theta^2} \right)^2 \mathrm{d}\theta. \tag{21}$$

We designate the splines created by minimizing (21) over all periodic piecewise cubic polynomials r that interpolate the data and have continuous derivatives at the nodes θ_i "polar second derivative L_2 splines". Since (21) is strictly convex, polar second derivative L_2 splines exist and are unique.

We define a "polar second derivative L_1 spline" to be the piecewise cubic polynomial that minimizes

$$\int_{\theta_0}^{\theta_I} \left| \frac{\mathrm{d}^2 r}{\mathrm{d}\theta^2} \right| \mathrm{d}\theta \tag{22}$$

over all periodic piecewise cubic polynomials r that interpolate the data and have continuous derivatives at the nodes θ_i. Polar second derivative L_1 splines exist because functional (22) is convex. However, polar second derivative L_1 splines are not necessarily unique for the same reasons that Cartesian second derivative L_1 splines are not necessarily unique (see Subsection 2.1 above and (Lavery, 2000)). To alleviate this problem, one adds regularization terms to the minimization principle to make it

$$\int_{\theta_0}^{\theta_I} \left| \frac{\mathrm{d}^2 r}{\mathrm{d}\theta^2} \right| \mathrm{d}\theta + \varepsilon \sum_{i=0}^{I-1} \left| \frac{\mathrm{d}r}{\mathrm{d}\theta}(\theta_i) \right|. \tag{23}$$

Functional (23) is still not strictly convex and can therefore achieve its minimum for more than one set of spline coefficients. However, standard interior-point algorithms, including the primal affine method used to minimize functional (23) to generate the computational results in the present paper and in (Lavery, 2000), do yield a unique set of spline coefficients that minimize (a discretization of) functional (23).

3.2. Polar curvature splines

In the research literature and in operational codes, polar-coordinate cubic splines based on curvature are often defined in the same way that Cartesian-coordinate cubic based on curvature have been defined, namely, by minimizing the arclength integral of the square of curvature. We adopt this approach and define a "polar curvature L_2 spline of type 1" to be a piecewise cubic polynomial that minimizes

$$\int_{\theta=\theta_0}^{\theta=\theta_I} (\kappa)^2 \, \mathrm{d}s \tag{24}$$

over all periodic piecewise cubic polynomials r that interpolate the data and have continuous derivatives at the nodes. For reference, the expression for curvature in polar coordinates is

$$\kappa = \frac{r^2 + 2(\frac{\mathrm{d}r}{\mathrm{d}\theta})^2 - r\frac{\mathrm{d}^2 r}{\mathrm{d}\theta^2}}{[r^2 + (\frac{\mathrm{d}r}{\mathrm{d}\theta})^2]^{3/2}} \tag{25}$$

and the arclength differential is

$$\mathrm{d}s = \left[r^2 + \left(\frac{\mathrm{d}r}{\mathrm{d}\theta}\right)^2\right]^{1/2} \mathrm{d}\theta. \tag{26}$$

Analysis of minimization of (24) over the finite-dimensional space of C^1-smooth cubic functions of interest in this paper has not yet been carried out. When it is carried out, it should be carried out in the context of analysis of all of the L_1 and L_2 curvature-based functionals introduced in this subsection and in Subsection 2.2. To promote existence, uniqueness and computational stability, we choose to add to functional (24) strictly convex regularization terms to obtain

$$\int_{\theta=\theta_0}^{\theta=\theta_I} (\kappa)^2 \,\mathrm{d}s + \varepsilon^2 \sum_{i=0}^{I-1} \left(\frac{\mathrm{d}r}{\mathrm{d}\theta}(\theta_i)\right)^2. \tag{27}$$

Functional (27) can be rewritten using (25) and (26) as

$$\int_{\theta_0}^{\theta_I} \frac{[r^2 + 2(\frac{\mathrm{d}r}{\mathrm{d}\theta})^2 - r\frac{\mathrm{d}^2 r}{\mathrm{d}\theta^2}]^2}{[r^2 + (\frac{\mathrm{d}r}{\mathrm{d}\theta})^2]^{5/2}} \,\mathrm{d}\theta + \varepsilon^2 \sum_{i=0}^{I-1} \left(\frac{\mathrm{d}r}{\mathrm{d}\theta}(\theta_i)\right)^2. \tag{28}$$

Functional (27) or, equivalently, (28) may have more than one local minimum and can therefore achieve its minimum for more than one set of spline coefficients. However, in all of the computational experiments carried out by the author, the variant of the Levenberg–Marquardt method (Dennis and Schnabel, 1983; Press et al., 1988) used to generate the curvature-based L_2 spline computational results in this paper yielded a unique set of spline coefficients that minimizes (a discretization of) functional (28).

In analogy to the polar curvature L_1 spline of type 2 to be introduced below and in analogy to the Cartesian curvature L_2 spline of type 2 introduced in the previous section, we define a "polar curvature L_2 spline of type 2" to be a periodic C^1-smooth piecewise cubic interpolant that minimizes

$$\int_{\theta_0}^{\theta_I} \frac{[r^2 + 2(\frac{\mathrm{d}r}{\mathrm{d}\theta})^2 - r\frac{\mathrm{d}^2 r}{\mathrm{d}\theta^2}]^2}{[r^2 + (\frac{\mathrm{d}r}{\mathrm{d}\theta})^2]^2} \,\mathrm{d}\theta + \varepsilon^2 \sum_{i=0}^{I-1} \left(\frac{\mathrm{d}r}{\mathrm{d}\theta}(\theta_i)\right)^2. \tag{29}$$

We define the L_1 analogues of polar curvature L_2 splines as follows. Taking the square roots of the integrand, ε^2 and the summand in functional (28), we define a "polar curvature L_1 spline of type 1" to be a periodic C^1-smooth piecewise cubic interpolant that minimizes

$$\int_{\theta_0}^{\theta_I} \frac{|r^2 + 2(\frac{\mathrm{d}r}{\mathrm{d}\theta})^2 - r\frac{\mathrm{d}^2 r}{\mathrm{d}\theta^2}|}{[r^2 + (\frac{\mathrm{d}r}{\mathrm{d}\theta})^2]^{5/4}} \,\mathrm{d}\theta + \varepsilon \sum_{i=0}^{I-1} \left|\frac{\mathrm{d}r}{\mathrm{d}\theta}(\theta_i)\right|. \tag{30}$$

We define a "polar curvature L_1 spline of type 2" to be a periodic C^1-smooth piecewise cubic interpolant that minimizes

$$\int_{\theta=\theta_0}^{\theta=\theta_I} |\kappa| \,\mathrm{d}s + \varepsilon \sum_{i=0}^{I-1} \left|\frac{\mathrm{d}r}{\mathrm{d}\theta}(\theta_i)\right| \tag{31}$$

or, equivalently,

$$\int_{\theta_0}^{\theta_I} \frac{|r^2 + 2(\frac{\mathrm{d}r}{\mathrm{d}\theta})^2 - r\frac{\mathrm{d}^2 r}{\mathrm{d}\theta^2}|}{r^2 + (\frac{\mathrm{d}r}{\mathrm{d}\theta})^2}\,\mathrm{d}\theta + \varepsilon \sum_{i=0}^{I-1} \left|\frac{\mathrm{d}r}{\mathrm{d}\theta}(\theta_i)\right|. \tag{32}$$

Just as was the case for Cartesian curvature L_1 splines, local and global existence and uniqueness properties of polar curvature L_1 splines are not yet known. However, in all of the computational experiments carried out by the author, the primal-affine-type method used to generate the curvature-based L_1 spline computational results in this paper yielded unique sets of spline coefficients that minimize (discretizations of) functionals (30) and (32).

4. Algorithms and computational results

We will present computational results for the 6 types of Cartesian-coordinate splines and the 6 types of polar-coordinate splines introduced above, namely,

1. Cartesian second derivative L_1 spline created by minimizing (7) with each integral on (x_i, x_{i+1}) discretized by a 100-subinterval midpoint rule and with $\varepsilon = 10^{-4}$.
2. Cartesian second derivative L_2 spline created by minimizing (6) with $p = 2$.
3. Cartesian curvature L_1 spline of type 1 created by minimizing (14) with each integral on (x_i, x_{i+1}) discretized by a 100-subinterval midpoint rule and with $\varepsilon = 10^{-4}$.
4. Cartesian curvature L_2 spline of type 1 created by minimizing (12) with each integral on (x_i, x_{i+1}) discretized by a 100-subinterval midpoint rule and with $\varepsilon = 10^{-4}$.
5. Cartesian curvature L_1 spline of type 2 created by minimizing (16) with each integral on (x_i, x_{i+1}) discretized by a 100-subinterval midpoint rule and with $\varepsilon = 10^{-4}$.
6. Cartesian curvature L_2 spline of type 2 created by minimizing (13) with each integral on (x_i, x_{i+1}) discretized by a 100-subinterval midpoint rule and with $\varepsilon = 10^{-4}$.
7. Polar second derivative L_1 spline created by minimizing (23) with each integral on (θ_i, θ_{i+1}) discretized by a 100-subinterval midpoint rule and with $\varepsilon = 10^{-4}$.
8. Polar second derivative L_2 spline created by minimizing (21).
9. Polar curvature L_1 spline of type 1 created by minimizing (30) with each integral on (θ_i, θ_{i+1}) discretized by a 100-subinterval midpoint rule and with $\varepsilon = 10^{-4}$.
10. Polar curvature L_2 spline of type 1 created by minimizing (28) with each integral on (θ_i, θ_{i+1}) discretized by a 100-subinterval midpoint rule and with $\varepsilon = 10^{-4}$.
11. Polar curvature L_1 spline of type 2 created by minimizing (32) with each integral on (θ_i, θ_{i+1}) discretized by a 100-subinterval midpoint rule and with $\varepsilon = 10^{-4}$.
12. Polar curvature L_2 spline of type 2 created by minimizing (29) with each integral on (θ_i, θ_{i+1}) discretized by a 100-subinterval midpoint rule and with $\varepsilon = 10^{-4}$.

The primal affine method, described in (Vanderbei et al., 1986; Vanderbei, 1989; Lavery, 2000, 2001), was used to minimize the second-derivative-based L_1 spline functionals. The curvature-based L_1 spline functionals were minimized by an adaption of the primal affine method in which the direction to the new interim solution is determined by solving a weighted least-squares system based on the Newton equations

and the weights for the next least-squares system are calculated using the residuals of the original overdetermined system. The second-derivative-based L_2 spline functionals, which are quadratic, were minimized by simply solving the corresponding linear system. The variant of the Levenberg–Marquardt algorithm (Dennis and Schnabel, 1983; Press et al., 1988) used to minimize the curvature-based L_2 spline functionals was based solely on the Newton equations and had a constant iterate-to-iterate updating factor.

The computational results for polar-coordinate L_1 and L_2 splines presented below are for the following very challenging multiscale data set with 33 data points on discontinuously connected straight lines, circular arcs, a trigonometric function and oscillatory curves:

$\theta_0 = 0$	$r_0 = 2$	$\theta_{17} = 2.879793266$	$r_{17} = 2.5$
$\theta_1 = 0.124354995$	$r_1 = 2.015564437$	$\theta_{18} = 3.141592654$	$r_{18} = 2.5$
$\theta_2 = 0.255341921$	$r_2 = 2.061552813$	$\theta_{19} = 3.228859117$	$r_{19} = 2.5$
$\theta_3 = 0.291456795$	$r_3 = 2.610076627$	$\theta_{20} = 3.665191430$	$r_{20} = 2.5$
$\theta_4 = 0.380506377$	$r_4 = 2.692582404$	$\theta_{21} = 3.926990817$	$r_{21} = 1$
$\theta_5 = 0.558599315$	$r_5 = 2.358495283$	$\theta_{22} = 4.014257281$	$r_{22} = 1.25$
$\theta_6 = 0.643501109$	$r_6 = 2.5$	$\theta_{23} = 4.101523742$	$r_{23} = 1$
$\theta_7 = 0.785398164$	$r_7 = 2.828427125$	$\theta_{24} = 4.188790204$	$r_{24} = 1.5$
$\theta_8 = 1.107148718$	$r_8 = 2.236067977$	$\theta_{25} = 4.276056667$	$r_{25} = 1$
$\theta_9 = 1.325817664$	$r_9 = 2.061552813$	$\theta_{26} = 4.363323131$	$r_{26} = 2$
$\theta_{10} = 1.570796327$	$r_{10} = 2$	$\theta_{27} = 4.712388980$	$r_{27} = 1$
$\theta_{11} = 1.665748034$	$r_{11} = 1.054751155$	$\theta_{28} = 4.974188368$	$r_{28} = 1.258819045$
$\theta_{12} = 1.951302704$	$r_{12} = 1.346291202$	$\theta_{29} = 5.235987756$	$r_{29} = 1.5$
$\theta_{13} = 2.158798931$	$r_{13} = 1.802775638$	$\theta_{30} = 5.497787144$	$r_{30} = 1.707106781$
$\theta_{14} = 2.279422599$	$r_{14} = 2.304886114$	$\theta_{31} = 5.759586532$	$r_{31} = 1.866025404$
$\theta_{15} = 2.312065376$	$r_{15} = 2.5$	$\theta_{32} = 6.021385919$	$r_{32} = 1.965925826$
$\theta_{16} = 2.617993878$	$r_{16} = 2.5$	$\theta_{33} = 6.283185308$	$r_{33} = 2.$

Since the data are assumed to be periodic, the last data point coincides with the zeroeth data point. The computational results for Cartesian-coordinate L_1 and L_2 splines presented below are for the data set given above in which each data point (θ_i, r_i) is interpreted as a Cartesian-coordinate data point (x_i, z_i). In this case, since the data are not intended to be periodic, the last data point is not interpreted as coinciding with the zeroeth data point. In the figures, the data points are denoted by $\times$.

In Figs. 1–6, we present L_1 and L_2 splines for the Cartesian-coordinate data set. There are large differences between L_1 and L_2 splines and between splines based on different minimization principles. Comparing Figs. 1 and 2, one immediately notes that the Cartesian second derivative L_1 spline preserves shape much better than the Cartesian second derivative L_2 spline, an observation consistent with the results in (Lavery, 2000). The Cartesian curvature L_1 splines in Figs. 3 and 5 have less overshoot and oscillation than the Cartesian second derivative L_1 spline on the left of the plots but slightly more at the data points in the interval $[4, 5]$. The Cartesian curvature L_2 splines in Figs. 4 and 6 have less overshoot and oscillation than the Cartesian second derivative L_2 spline of Fig. 1 but still have a lot more overshoot and oscillation than the Cartesian curvature L_1 splines of Figs. 4 and 6.

In Figs. 7–12, we present L_1 and L_2 splines for the polar-coordinate data set described above. Again, there are large differences between L_1 and L_2 splines and between splines based on different minimization principles. The polar curvature L_1 splines in Figs. 9 and 11 preserve shape better than the

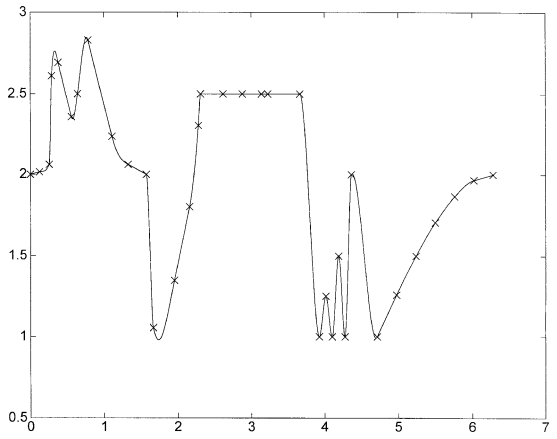

Fig. 1. Cartesian second derivative L_1 spline based on (7).

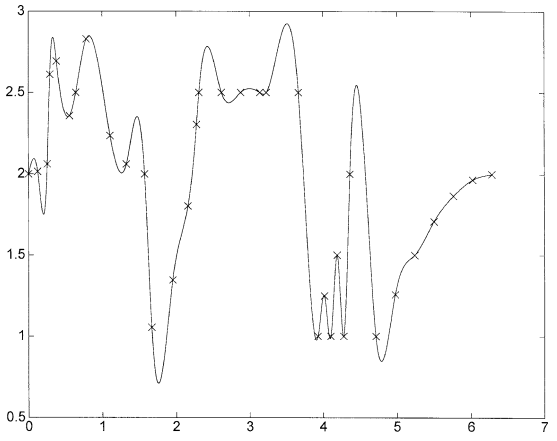

Fig. 2. Cartesian second derivative L_2 spline based on (6) with $p = 2$.

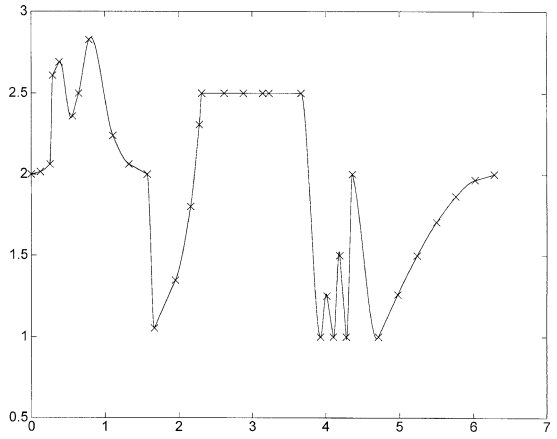

Fig. 3. Cartesian curvature L_1 spline of type 1 based on (14).

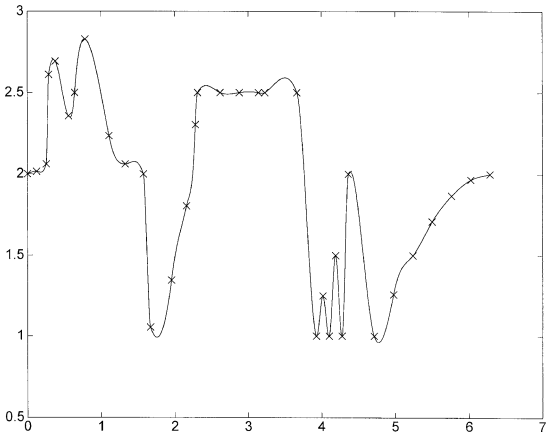

Fig. 4. Cartesian curvature L_2 spline of type 1 based on (12).

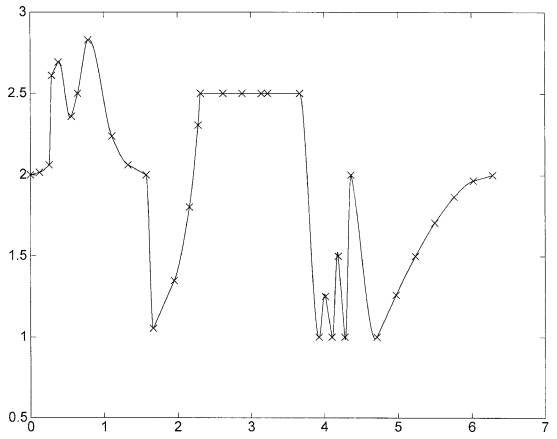

Fig. 5. Cartesian curvature L_1 spline of type 2 based on (16).

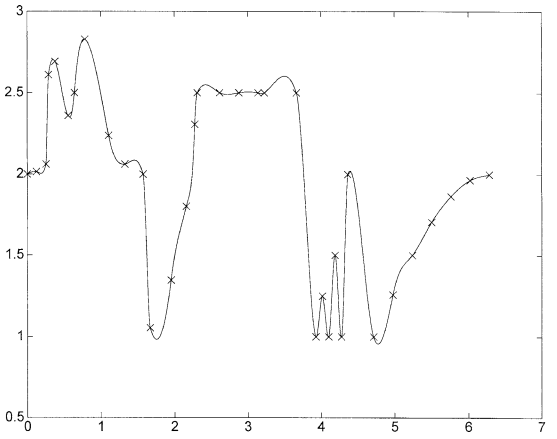

Fig. 6. Cartesian curvature L_2 spline of type 2 based on (13).

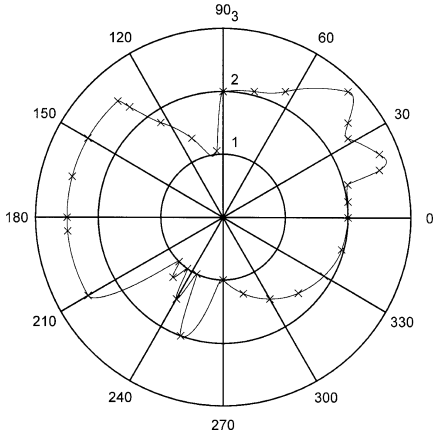

Fig. 7. Polar second derivative L_1 spline based on (23).

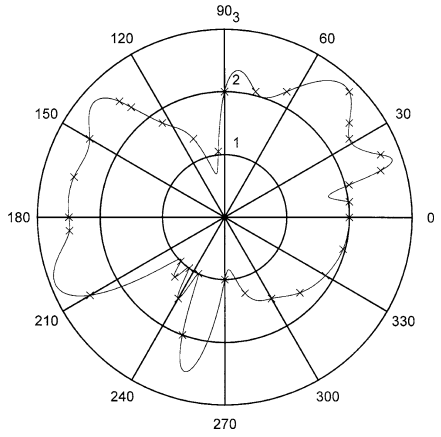

Fig. 8. Polar second derivative L_2 spline based on (21).

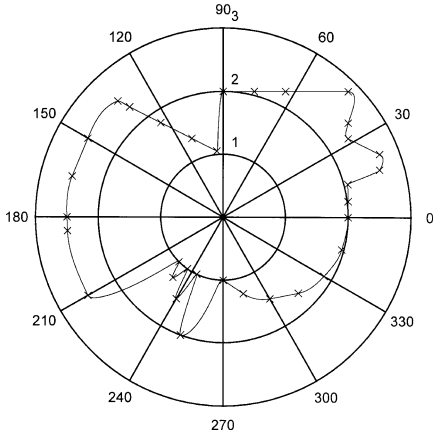

Fig. 9. Polar curvature L_1 spline of type 1 based on (30).

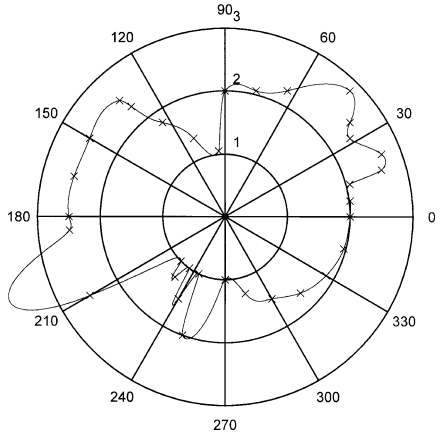

Fig. 10. Polar curvature L_2 spline of type 1 based on (28).

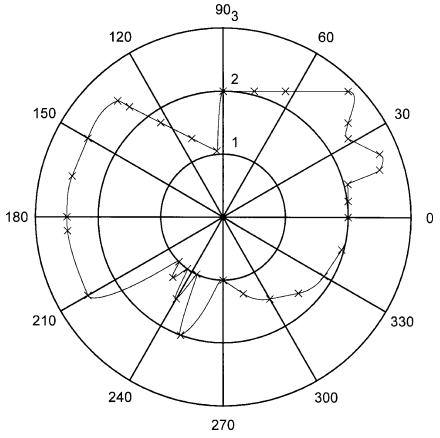

Fig. 11. Polar curvature L_1 spline of type 2 based on (32).

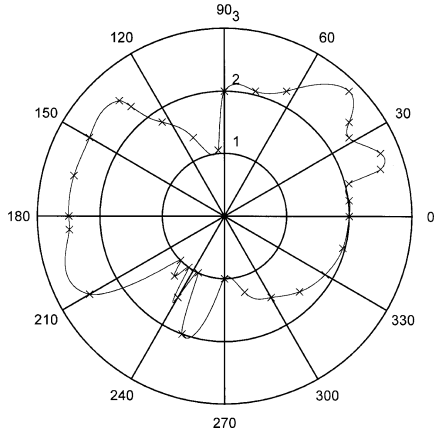

Fig. 12. Polar curvature L_2 spline of type 2 based on (29).

polar second derivative L_1 spline in Fig. 7. The L_1 splines in Figs. 7, 9 and 11 all preserve shape much better than the L_2 splines in Figs. 8, 10 and 12. It is worth noting that the polar curvature L_2 spline of type 1 in Fig. 10 is particularly poor at preserving shape. This information is of considerable value, since this type of spline has previously been the most common choice for curvature-based splines in geometric modeling applications.

The computational results presented here suggest that changing the function space of the minimization principle from L_2 to L_1 is a large factor in improving the shape-preserving properties of splines. In polar coordinates, shifting from a minimization principle based on the second derivative to one based on curvature is also a large factor. It is worth noting that the "overshoot" near oscillatory data of the Cartesian curvature L_1 splines in Figs. 3 and 5 is partly an artifact of human perception. In Cartesian coordinates, the observer often associates vertical and horizontal with the typical vertical and horizontal directions of everyday life. Curvature-based splines, which are independent of the coordinate system, are best suited for a framework in which there is little or no differentiation between vertical and horizontal directions. Even though, in polar coordinates, vertical and horizontal could be associated with radial and angular directions (for example, when modeling cross sections of planets and stars), most observers interested in geometric modeling do not make such an association. Curvature-based cubic L_1 splines are well suited for shape-preserving modeling in polar coordinate systems, much more so than second-derivative-based cubic L_1 splines (compare Figs. 9 and 11 to Fig. 7). Much further investigation is, of course, needed before one can fully characterize under what circumstances curvature-based cubic L_1 splines preserve shape better than alternative types of L_1 and L_2 splines.

One interesting capability of polar curvature L_1 splines is their ability to interpolate data lying on straight lines by curves that are, to within visual accuracy, also straight lines. Note in Figs. 9 and 11 the apparent straight-line nature of the L_1 splines between (θ_7, r_7) and (θ_{10}, r_{10}) and between (θ_{11}, r_{11}) and (θ_{15}, r_{15}). These L_1 splines are, of course, not exactly straight lines between these points because, in polar coordinates, a straight line is represented by

$$r = \frac{1}{c_1 \cos\theta + c_2 \sin\theta} \tag{33}$$

for constants c_1 and c_2. The local basis for L_1 splines introduced in this paper consists only of powers of θ and does not include reciprocals of trigonometric functions. Nevertheless, curvature-based L_1 splines do well in approximating straight lines by cubic polynomials in θ. For example, in the interval from θ_7 to θ_8 the vertical error of the spline vs. the straight line segment connecting the two data points is bounded by 0.00221 for the L_1 spline of type 1 in Fig. 9 and by 0.00228 for the L_1 spline of type 2 in Fig. 11. When coupled with a curvature-based L_1 minimization principle, piecewise cubic interpolants, which have an undeserved reputation for inflexibility, perform in a flexible, shape-preserving, multiscale manner.

To close this section, we comment here on CPU times required for computing the various splines. CPU times on a Gateway personal computer running under Microsoft Visual C++ Version 6.0 are given in Table 1 for the Cartesian splines of Figs. 1–6 and in Table 2 for the polar splines of Figs. 7–12.

The research codes that produced these CPU times were not optimized for algorithmic efficiency or run-time performance. The CPU times in the tables above are therefore only indicators of relative orders of magnitude. Classical second-derivative-based L_2 splines (Figs. 2 and 8) are by far the least expensive of the splines investigated here. However, such splines are of little use when shape preservation is an issue. In order of magnitude, the CPU times for curvature-based L_1 splines are comparable to those for second-derivative-based L_1 splines (larger by factors of 1.6–3.7) and comparable to those for

Table 1
CPU times for the Cartesian splines of Figs. 1–6

	L_1	L_2
Cartesian second derivative spline	0.186 sec (Fig. 1)	0.005 sec (Fig. 2)
Cartesian curvature spline of type 1	0.693 sec (Fig. 3)	0.821 sec (Fig. 4)
Cartesian curvature spline of type 2	0.510 sec (Fig. 5)	0.559 sec (Fig. 6)

Table 2
CPU times for the polar splines of Figs. 7–12

	L_1	L_2
Polar second derivative spline	0.299 sec (Fig. 7)	0.008 sec (Fig. 8)
Polar curvature spline of type 1	0.519 sec (Fig. 9)	1.114 sec (Fig. 10)
Polar curvature spline of type 2	0.466 sec (Fig. 11)	1.076 sec (Fig. 12)

curvature-based L_2 splines (smaller by factors of 1.1–2.3). It is practically certain that in the future more efficient nonlinear programming algorithms will be developed for polar curvature L_1 and L_2 splines. If the computational cost of L_1 splines turns out to be comparable to that of L_2 splines, then L_1 splines will be preferred over L_2 splines for many polar coordinate modeling tasks in which shape preservation is an issue.

5. Rationale for curvature-based cubic L_1 splines

For many types of data, coordinate systems and tasks, the best subgrid model that one can establish for behavior in the region between two data points is a straight line. Connecting points by straight line segments always preserves shape, although it does not in general produce a smooth curve and is therefore deficient for many geometric modeling tasks.

The rationale behind curvature-based L_1 splines is that the spline minimization principle should drive the curve toward straight line segments that connect the data points. In Cartesian coordinates, a straight line has both second derivative and curvature equal to zero. Thus, in Cartesian coordinates, L_1 minimization principles such as (7), (14) and (16), which correspond to (approximately) solving the equations

$$z'' = 0, \tag{34}$$

$$\frac{z''}{[1+(z')^2]^{5/4}} = \kappa \cdot \left[1+(z')^2\right]^{1/4} = 0, \tag{35}$$

$$\frac{z''}{1+(z')^2} = \kappa \cdot \left[1+(z')^2\right]^{1/2} = 0, \tag{36}$$

respectively, in the L_1 norm, all perform well. In polar coordinates, a straight line does have zero curvature but does not have second derivative with respect to θ equal to zero. Polar-coordinate functions with zero second derivative are linear in θ and are therefore spirals. It is thus not surprising that polar

second derivative L_1 splines, which are based on minimizing (23), that is, on (approximately) solving the equation

$$\frac{\mathrm{d}^2 r}{\mathrm{d}\theta^2} = 0 \tag{37}$$

in the L_1 norm, do not preserve shape well. In contrast, polar curvature L_1 splines, which are based on minimizing (30) and (32), that is, on (approximately) solving the equations

$$\frac{r^2 + 2(\frac{\mathrm{d}r}{\mathrm{d}\theta})^2 - r\frac{\mathrm{d}^2 r}{\mathrm{d}\theta^2}}{[r^2 + (\frac{\mathrm{d}r}{\mathrm{d}\theta})^2]^{5/4}} = \kappa \cdot \left[r^2 + \left(\frac{\mathrm{d}r}{\mathrm{d}\theta}\right)^2\right]^{1/4} = 0, \tag{38}$$

$$\frac{r^2 + 2(\frac{\mathrm{d}r}{\mathrm{d}\theta})^2 - r\frac{\mathrm{d}^2 r}{\mathrm{d}\theta^2}}{r^2 + (\frac{\mathrm{d}r}{\mathrm{d}\theta})^2} = \kappa \cdot \left[r^2 + \left(\frac{\mathrm{d}r}{\mathrm{d}\theta}\right)^2\right]^{1/2} = 0 \tag{39}$$

in the L_1 norm, do preserve shape well because they drive the curvature (times a nonzero factor) toward 0 and therefore the spline toward straight-line segments.

6. Other types of polar-coordinate cubic L_1 and L_2 splines

In addition to investigating the polar-coordinate cubic L_1 splines introduced in Sections 2 and 3, the author investigated polar-coordinate cubic L_1 splines based on the minimization principles

$$\int_{\theta_0}^{\theta_I} \frac{|r^2 + 2(\frac{\mathrm{d}r}{\mathrm{d}\theta})^2 - r\frac{\mathrm{d}^2 r}{\mathrm{d}\theta^2}|}{[r^2 + (\frac{\mathrm{d}r}{\mathrm{d}\theta})^2]^{3/2}}\,\mathrm{d}\theta + \varepsilon \sum_{i=0}^{I-1} \left|\frac{\mathrm{d}r}{\mathrm{d}\theta}(\theta_i)\right|, \tag{40}$$

$$\int_{\theta_0}^{\theta_I} \left|r^2 + 2\left(\frac{\mathrm{d}r}{\mathrm{d}\theta}\right)^2 - r\frac{\mathrm{d}^2 r}{\mathrm{d}\theta^2}\right| \mathrm{d}\theta + \varepsilon \sum_{i=0}^{I-1} \left|\frac{\mathrm{d}r}{\mathrm{d}\theta}(\theta_i)\right|, \tag{41}$$

$$\int_{\theta_0}^{\theta_I} \left|\rho r + 2\left(\frac{d\rho}{\mathrm{d}\theta}\right)\left(\frac{\mathrm{d}r}{\mathrm{d}\theta}\right) - \rho\frac{\mathrm{d}^2 r}{\mathrm{d}\theta^2}\right| \mathrm{d}\theta + \varepsilon \sum_{i=0}^{I-1} \left|\frac{\mathrm{d}r}{\mathrm{d}\theta}(\theta_i)\right|, \tag{42}$$

$$\int_{\theta_0}^{\theta_I} \left|\frac{\mathrm{d}^2 r}{\mathrm{d}\theta^2} - \frac{\mathrm{d}^2 \rho}{\mathrm{d}\theta^2}\right| \mathrm{d}\theta + \varepsilon \sum_{i=0}^{I-1} \left|\frac{\mathrm{d}r}{\mathrm{d}\theta}(\theta_i)\right|, \tag{43}$$

$$\int_{\theta_0}^{\theta_I} |r - \rho|\,\mathrm{d}\theta + \varepsilon \sum_{i=0}^{I-1} \left|\frac{\mathrm{d}r}{\mathrm{d}\theta}(\theta_i)\right|, \tag{44}$$

where ρ denotes the straight-line segments

$$\rho(\theta) = \frac{r_i r_{i+1} \sin(\theta_i - \theta_{i+1})}{(r_{i+1}\cos\theta_{i+1} - r_i \cos\theta_i)\sin\theta - (r_{i+1}\sin\theta_{i+1} - r_i \sin\theta_i)\cos\theta} \tag{45}$$

that connect consecutive data points (θ_i, r_i) and (θ_{i+1}, r_{i+1}). Functional (40) was investigated because it is equal to

$$\int_{\theta_0}^{\theta_I} |\kappa| \, \mathrm{d}\theta + \varepsilon \sum_{i=0}^{I-1} \left| \frac{\mathrm{d}r}{\mathrm{d}\theta}(\theta_i) \right|. \tag{46}$$

The integrand inside the absolute value in functional (41) is the numerator of polar-coordinate curvature. This minimization principle was investigated because it is a polar-coordinate analogue of the standard Cartesian-coordinate minimization principle (6) with $p = 2$ (in both cases, the numerator of curvature is used as the basis for the minimization principle). Minimization principle (42) was investigated because it is a "linearization" of (41). Minimization principles (43) and (44) were investigated because, by minimizing the L_1 norm of the second or zeroeth derivative of the spline minus the second or zeroeth derivative of the straight-line segments that connect the data points, one might hope to obtain interpolants that would stay close to straight-line segments and therefore preserve shape.

L_1 splines based on minimizing (40) performed similar to polar curvature L_1 splines of types 1 and 2 and preserved shape well. None of the L_1 splines based on minimizing (41), (42), (43) or (44) preserved shape well. The author also investigated polar-coordinate L_2 splines based on L_2 analogues of minimization principles (40)–(44) in which the integrands, ε and the summands were squared. These L_2 splines all preserved shape less well than their L_1 counterparts.

7. Extensions

Extension of polar curvature L_1 splines to univariate curvature-based L_1 splines in general curvilinear coordinate systems will be an important area of research. The curvilinear coordinate systems that need to be considered are not only classical curvilinear coordinate systems but also curvilinear coordinate systems created numerically for complicated geometries. One will probably find that there will be limitations on what can be interpolated by splines in coordinate systems that have regions of high curvature. Determining the relationship between the spline grid, the minimization principle and the curvilinear coordinate system will be a critical aspect of this research.

Curvature-based interpolation of bivariate data in spherical, elliptical and computationally constructed coordinate systems and eventually of multivariate data will involve extending the results for Cartesian second derivative bivariate cubic L_1 splines (Lavery, 2001) to curvature-based settings. A critical issue in this research will be what types of two- or higher-dimensional curvature should be used to replace the second derivatives of the Cartesian-coordinate L_1 minimization principles.

Polynomial splines will not fit all needs and, in particular, are not appropriate when exact representation of straight lines in polar coordinates (by reciprocals of trigonometric functions) is desired. It can be hypothesized that splines constructed using nonpolynomial local basis functions will also exhibit enhanced shape-preservation properties if their coefficients are computed using a curvature-based L_1 minimization principle.

8. Conclusion

Changing the L_2 norm to the L_1 norm and using curvature rather than the second derivative in the spline minimization principle have surprisingly large influence on the shape-preserving properties of splines, especially in polar coordinates. While curvature-based cubic L_1 splines will not fit all geometric modeling needs, they do provide a new option that has wide applicability. The discovery that it is computationally feasible to compute shape-preserving splines by minimizing the L_1 norm of curvature provides the basis for much future theoretical and computational research that may lead to large payoffs in improved geometric modeling.

References

Alfeld, P., Neamtu, M., Schumaker, L.L., 1995. Circular Bernstein–Bézier polynomials, in: Dæhlen, M., Lyche, T., Schumaker, L.L. (Eds.), Mathematical Methods for Curves and Surfaces. Vanderbilt University Press, Nashville, TN, pp. 11–20.

Burmeister, W., Heß, W., Schmidt, J.W., 1985. Convex spline interpolants with minimal curvature. Computing 35, 219–229.

Casciola, G., Morigi, S., 1997. Spline curves in polar and Cartesian coordinates, in: Le Méhauté, A., Rabut, C., Schumaker, L.L. (Eds.), Curves and Surfaces with Applications in CAGD. Vanderbilt University Press, Nashville, TN, pp. 61–68.

de Casteljau, P., 1994. Splines focales, in: Laurent, P.-J., Le Méhauté, A., Schumaker, L.L. (Eds.), Curves and Surfaces in Geometric Design. A. K. Peters, Wellesley, MA, pp. 91–103.

Dennis, J.E. Jr., Schnabel, R.B., 1983. Numerical Methods for Unconstrained Optimization and Nonlinear Equations. Prentice-Hall, Englewood Cliffs, NJ.

Fisher, S.D., Jerome, J.W., 1976. Stable and unstable elastica equilibrium and the problem of minimum curvature. J. Math. Anal. Appl. 53, 367–376.

Golomb, M., 1968. Approximation by periodic spline interpolants on uniform meshes. J. Approx. Theory 1, 26–65.

Golomb, M., Jerome, J.W., 1982. Equilibria of the curvature functional and manifolds of nonlinear interpolating spline curves. SIAM J. Math. Anal. 13, 421–458.

Goodman, T.N.T., Lee, S.L., 1984. B-splines on the circle and trigonometric B-splines, in: Singh, S.P, Burry, J.H.W., Watson, B. (Eds.), Approximation Theory and Spline Functions. Reidel, Dordrecht, pp. 297–325.

Jerome, J.W., 1973a. Minimization problems and linear and nonlinear spline functions. I: Existence. SIAM J. Numer. Anal. 10, 808–819.

Jerome, J.W., 1973b. Minimization problems and linear and nonlinear spline functions. II: Convergence. SIAM J. Numer. Anal. 10, 820–830.

Jerome, J.W., 1975. Smooth interpolating curves of prescribed length and minimum curvature. Proc. Amer. Math. Soc. 51, 62–66.

Lavery, J.E., 2000. Univariate cubic L_p splines and shape-preserving, multiscale interpolation by univariate cubic L_1 splines. Computer Aided Geometric Design 17, 319–336.

Lavery, J.E., 2001. Shape-preserving, multiscale interpolation by bi- and multivariate cubic L_1 splines. Computer Aided Geometric Design. To appear.

Linner, A., 1996. Unified representations of nonlinear splines. J. Approx. Theory 84, 315–350.

Lyche, T., 1999. Trigonometric splines: a survey with new results, in: Pena, J.M. (Ed.), Shape Preserving Representations in Computer Aided Geometric Design. Nova Science Publishers, New York, pp. 201–227.

Lyche, T., Winther, R., 1979. A stable recurrence relation for trigonometric B-splines. J. Approx. Theory 25, 266–279.

Press, W.H., Flannery, B.P., Teukolsky, S.A., Vetterling, W.T., 1988. Numerical Recipes in C: The Art of Scientific Computing. Cambridge University Press, Cambridge.

Sanchez-Reyes, J., 1992. Single-valued spline curves in polar coordinates. Computer Aided Design 24, 307–315.

Schumaker, L.L., 1981. Spline Functions: Basic Theory. Wiley-Interscience, New York.

Vanderbei, R.J., 1989. Affine-scaling for linear programs with free variables. Math. Programming 43, 31–44.

Vanderbei, R.J., Meketon, M.J., Freedman, B.A., 1986. A modification of Karmarkar's linear programming algorithm. Algorithmica 1, 395–407.